Infectious Medicine 3 (2024) 100143

Contents lists available at ScienceDirect

Infectious Medicine

journal homepage: www.elsevier.com/locate/imj

Original Article

Diagnostic and prognostic value of disulfidptosis-related genes in sepsis

Wenlu Zou, Lintao Sai, Wen Sai, Li Song, Gang Wang*

Department of Infectious Disease, Qilu Hospital, Cheeloo College of Medicine, Shandong University, Jinan 250012, Shandong Province, China

A B S T R A C T

Background: Sepsis is a disease associated with high morbidity and mortality rates, especially among the elderly and patients in intensive care units. Disulfidptosis, a newly identified form of cell death triggered by disulfide stress, is emerging as a significant factor in disease progression. This study aimed to explore the diagnostic and prognostic value of disulfidptosis-related genes in sepsis.

Methods: We obtained two datasets from the Gene Expression Omnibus (GEO) database to conduct our analysis. Functional enrichment analysis was performed to identify relevant biological pathways. A protein-protein interaction network was constructed to identify hub genes critical to sepsis. Additionally, we analyzed the immune infiltration status in sepsis patients. The diagnostic value of these hub genes for sepsis was evaluated using nomograms, receiver operating characteristic (ROC) curves, and calibration curves in both training and validation datasets. Finally, a miRNA-immune-related hub genes (miRNA-IHGs) regulatory network was developed to elucidate the synergistic interactions between miRNAs and their target genes.

Results: A total of 3,469 differentially expressed genes (DEGs) were identified, of which seven were related to disulfidptosis (DR-DEGs). Functional enrichment analysis showed that DR-DEGs were significantly enriched in pathways related to actin dynamics. Five hub genes (MYH10, ACTN4, MYH9, FLNA, and IQGAP1) were identified as central to these processes. The analysis of immune infiltration revealed significantly lower levels of 11 immune cell types, while macrophages and regulatory T cells were significantly elevated in sepsis patients. The area under the ROC curves (AUCs) of the IHGs risk prediction model were 0.917 and 0.894 for the training and validation sets, respectively. A miRNA-IHGs regulatory network, comprising 17 nodes and 27 edges, was constructed, with MYH9 being the most frequently regulated by miRNAs.

Conclusion: The pathophysiological process of sepsis appears to involve disulfidptosis, highlighting it as a potential new therapeutic targets for sepsis management.

1. Introduction

Sepsis is a common, often fatal, and expensive disease in the general population, associated with high rates of mortality and morbidity. It is estimated that sepsis affects 30 million people worldwide each year, and its prevalence is increasing as the population ages [1]. In many countries, the true incidence of sepsis is difficult to determine due to underreporting, which remains a significant issue. Sepsis continues to pose a substantial burden on healthcare systems and insurance, especially in developing countries [2]. Research focused on diagnostic technologies that improve individualized management strategies and identify new biological targets offers the best hope for improving sepsis outcomes [3].

Disulfidptosis, a newly identified form of cell death proposed by Junjie Chen and Boyi Gan in 2023, is characterized by the susceptibility of the actin cytoskeleton to disulfide stress [4]. This type of cell death is closely associated with tumor progression and has been used in clinical oncology for prognosis prediction and as a therapeutic target [5–7]. Emerging evidence suggests a potential relationship between sepsis and actin cytoskeleton dynamics. In neutrophils, actin cytoskeleton remodeling is critical for their recruitment and migration to infection sites [8]. F-actin is essential for the contractility and function of

Abbreviations: GEO, gene expression omnibus; ROC, receiver operating characteristic; miRNA-IHGs, microRNA-immune related hub genes; DEGs, differentially expressed genes; DR-DEGs, disulfidptosis-related differentially expressed genes; NET, neutrophil extracellular trap; DRGs, disulfidptosis-related genes; GO, genome ontology; KEGG, Kyoto encyclopedia of genes; BP, biological process; CC, cellular component; MF, molecular function; ssGSEA, single-sample gene set enrichment analysis; IHGs, immune-related hub genes; MYH10, myosin heavy chain 10; ACTN4, alpha-actinin-4; MYH9, myosin heavy chain 9; FLNA, filamin-A; IQGAP1, Iq motif containing GTPase activating protein 1; aDCs, activated dendritic cells; iDCs, immature dendritic cells; pDCs, plasmacytoid dendritic cells; Tfh, follicular helper T cells; TIL, tumor-infiltrating lymphocytes; Treg, regulatory T cells; CCR, CC chemokine; HLA, human leukocyte antigen; APC co-inhibition, antigen-presenting cell co-inhibition; FOXP3, forkhead box P3.

* Corresponding author.
E-mail address: wginfection@email.sdu.edu.cn (G. Wang).

https://doi.org/10.1016/j.imj.2024.100143
Received 22 April 2024; Received in revised form 17 July 2024; Accepted 26 August 2024

various organs, including the heart and lungs, and disruption in F-actin organization and contractility during sepsis can lead to organ dysfunction and failure [9]. A key feature of sepsis is the formation of neutrophil extracellular trap (NET), which is regulated by the actin cytoskeleton. Inhibition of Arp 2/3-dependent F-actin polymerization not only reduces NET formation but also protects against pathological inflammation and tissue damage in septic lung injury [10].

To date, no studies have investigated the association between disulfidptosis and sepsis. Understanding the underlying mechanisms of disulfidptosis in sepsis could reveal novel therapeutic targets for treating this condition. In the present study, we used the NCBI Gene Expression Omnibus to identify differentially expressed genes (DEGs) in sepsis patients compared to healthy controls and screened for disulfidptosis-related hub genes using a combined dataset. We then analyzed differences in immune cell populations and immune functions between the two groups. Finally, we validated the diagnostic value of immune-related hub genes (IHGs) in both training and validation sets, providing insights into potential therapeutic strategies for sepsis.

2. Materials and methods

2.1. Data acquisition

The study flowchart is shown in Fig. 1. Microarray datasets were downloaded from the NCBI Gene Expression Omnibus (GEO) (https://www.ncbi.nlm.nih.gov/geo/) through a manual search [11], specifically GSE95233 (training set) and GSE57065 (validation set). The search keywords were “sepsis”, with the following searching strategies: (“sepsis”[MeSH Terms] OR sepsis [All Fields]) AND “Homo sapiens”[porgn] AND (“gse”[Filter] AND “Expression profiling by array”[Filter]). GSE95233 consisted of 102 sepsis samples derived from whole blood and 22 healthy samples, while

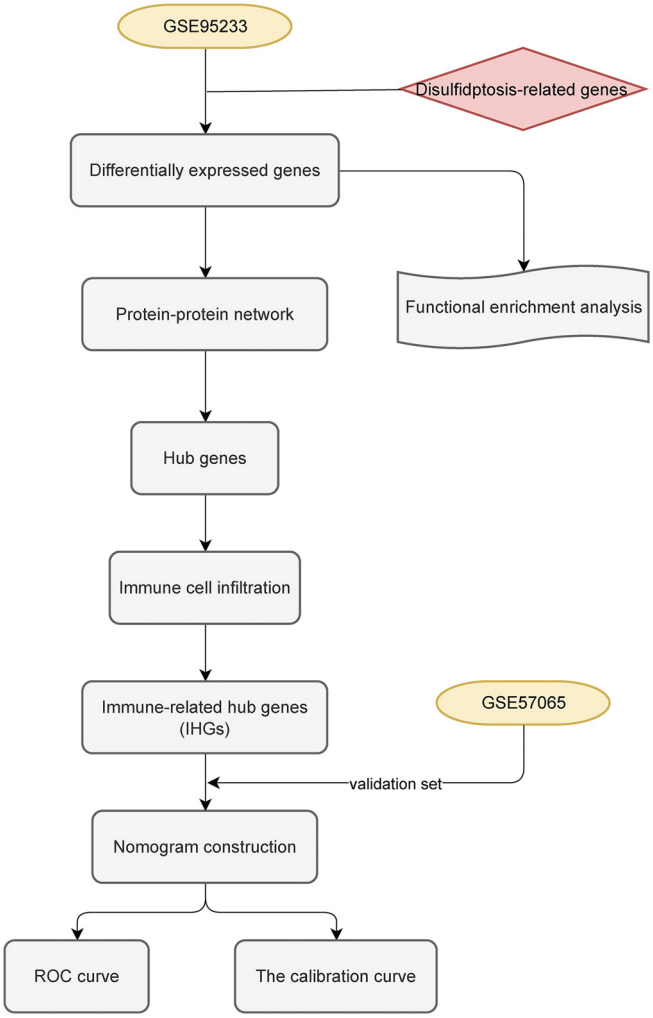

Fig. 1. Flowchart of the research.

GSE57065 included 82 sepsis patients and 25 normal blood samples.

2.2. Data processing and identification of differentially expressed genes

Disulfidptosis-related genes (DRGs) were sourced from a previous study [4], with a total of 14 DRGs included: ACTN4, ACTB, CD2AP, CAPZB, DSTN, FLNA, FLNB, INF2, IQGAP1, MYH10, MYL6, MYH9, PDLIM1, and TLN1. The two datasets were preprocessed using R (version 4.2.1). The "limma" package was used to identify DEGs [12]. The cutoffs for selecting DEGs were set at an adjusted p-value < 0.05 and $|\log_2$-fold change (FC)$|$ > 0.5. A Venn plot was used to show the intersection of DEGs and DRGs.

2.3. Functional enrichment analysis

The "Org.Hs.eg.db" R package was used to convert gene names to gene IDs. Functional enrichment analyses, including Genome-Ontology (GO) and Kyoto Encyclopedia of Genes (KEGG) pathway analyses, were implemented using the "ClusterProfiler" software package in R. The GO pathway analysis encompassed Biological Process (BP), Cellular Component (CC), and Molecular Function (MF). The results were visualized using the "enrichplot" and "ggplot2" R packages.

2.4. Protein–protein interaction (PPI) network construction and hub gene screening

The STRING online database (https://string-db.org/) was used to construct a PPI network for disulfidptosis-related DEGs, and Cytoscape software (version 3.9.1) was employed to process and extract key subnetwork. Five hub genes with the highest scores were selected using the maximum correlation criterion (MCC algorithm) via the cytoHubba plugin in Cytoscape.

2.5. Landscape of immune infiltration status

The single-sample Gene Set Enrichment Analysis (ssGSEA) algorithm was applied to calculate enrichment scores. The "GSVA" and "GSEABase" packages in R were used to quantify the scores of 16 immune cells and 13 immune-related pathways, exploring the relationship between disulfidptosis-related genes and immune cell infiltration. Heatmaps were displayed using the "pheatmap" package, and box plots were generated with the "ggpubr" and "reshape 2″ packages. The correlation heatmap of immune cells and immune function was depicted using the "corrplot" package. Spearman correlation analysis was conducted using the "psych" and "ggcorrplot" packages in R. IHGs were defined as those showing more than 50% immune infiltration and a correlation coefficient greater than 0.3.

2.6. Construction and validation of the IHGs risk prediction model

The IHGs nomogram was constructed using the "rms" R package. The accuracy of the nomogram was evaluated using the C-index and ROC curve through the "ROCR" package, and a calibration curve was plotted to verify its reliability.

2.7. MiRNA (microRNA)-IHGs regulatory network construction

The Enrichr database's TargetScan (https://maayanlab.cloud/Enrichr/) was used to predict miRNAs related to IHGs, retaining only Homo sapiens. The microRNA-immune related hub genes (miRNA-IHGs) regulatory network was visualized using Cytoscape software.

2.8. Statistical analysis

All data and statistical analyses were performed using R software (version 4.2.1). The Wilcox test or t-test was used to compare the statistical difference between the two groups. The unpaired student's t-test was used to calculate p-values and adjusted p-values, with p-values adjusted for false discovery rates (FDR). The relationship between the expression levels of genes associated with hub disulfidptosis and immune cells was analyzed by the Spearman correlation. Receiver operating characteristic (ROC) curves were used to assess the diagnostic accuracy of the three hub genes, with results expressed as the area under the ROC curves (AUROC) and a 95% confidence interval (CI). p-values were two-sided, and a p-value<0.05 were considered statistically significant.

3. Results

3.1. Screening for differentially expressed genes in disulfidptosis-related genes (DRGs)

A total of 3,469 DEGs were identified using the GSE95233 dataset, which included 102 sepsis and 22 normal samples. Of these, 1,719 genes were over-expressed, and 1,715 genes were under-expressed. The volcano plot and heatmap are presented in Fig. 2A and B, respectively. Seven DRGs (DR-DEGs) overlapped with these DEGs, including two up-regulated and five down-regulated genes (Fig. 2C). The clustering heatmap and volcano plot for DR-DEGs are shown in Fig. 2D and E.

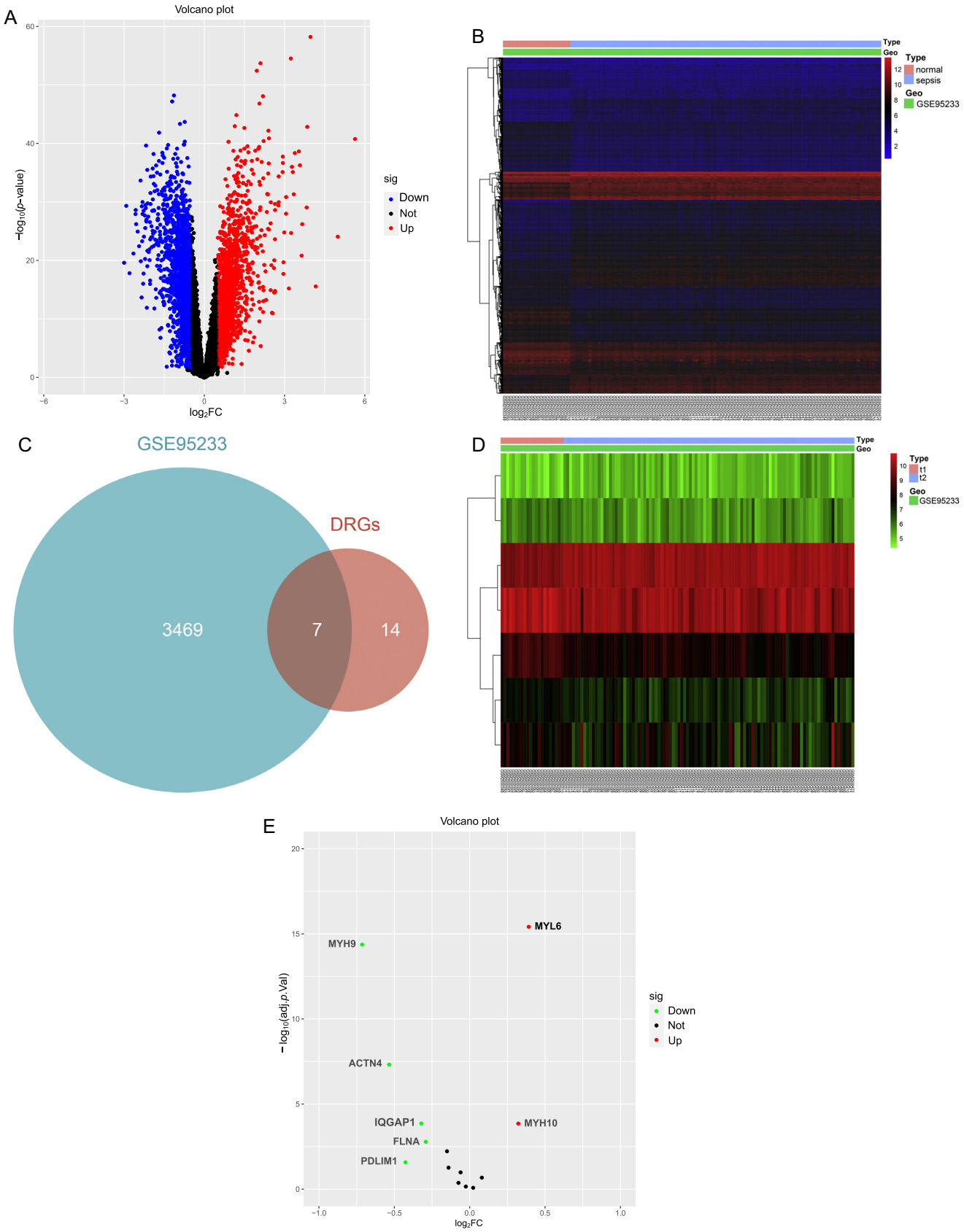

Fig. 2. Overview of DEGs in sepsis and normal patients. (A) Volcano plot of DEGs between normal and sepsis patients in the GSE95233 database. Red circles indicate up-regulated genes in sepsis, while blue circles indicate down-regulated genes in sepsis. (B) Heatmap for DEGs identified from the GSE95233 database. Each column represents one sample, and each row represents one DEG. (C) Venn diagram showing overlapping genes between DEGs and DRGs. (D) Heatmap of DR-DEGs. (E) Volcano plot of DR-DEGs.

3.2. Functional correlation analysis of DR-DEGs

In the KEGG analysis, DR-DEGs were primarily associated with the "Tight junction" and "Regulation of actin cytoskeleton" pathways (Fig. 3A). GO analysis for DR-DEGs included BP, CC, and MF (Fig. 3B). In the GO-BP analyses, the major enriched pathways were "actin filament-based movement" and "regulation of cell morphogenesis". In the GO-CC analysis, DR-DEGs were enriched in the "actin filament bundle" pathway. In the GO-MF analysis, DR-DEGs were associated with "actin binding" and "actin filament binding" pathways. Overall, DR-DEGs were significantly linked to actin dynamics-related pathways.

3.3. PPI network and hub genes

The PPI network included seven nodes and 15 edges (Fig. 4A). The minimum required interaction score was set at 0.4 using the STRING online database. All seven

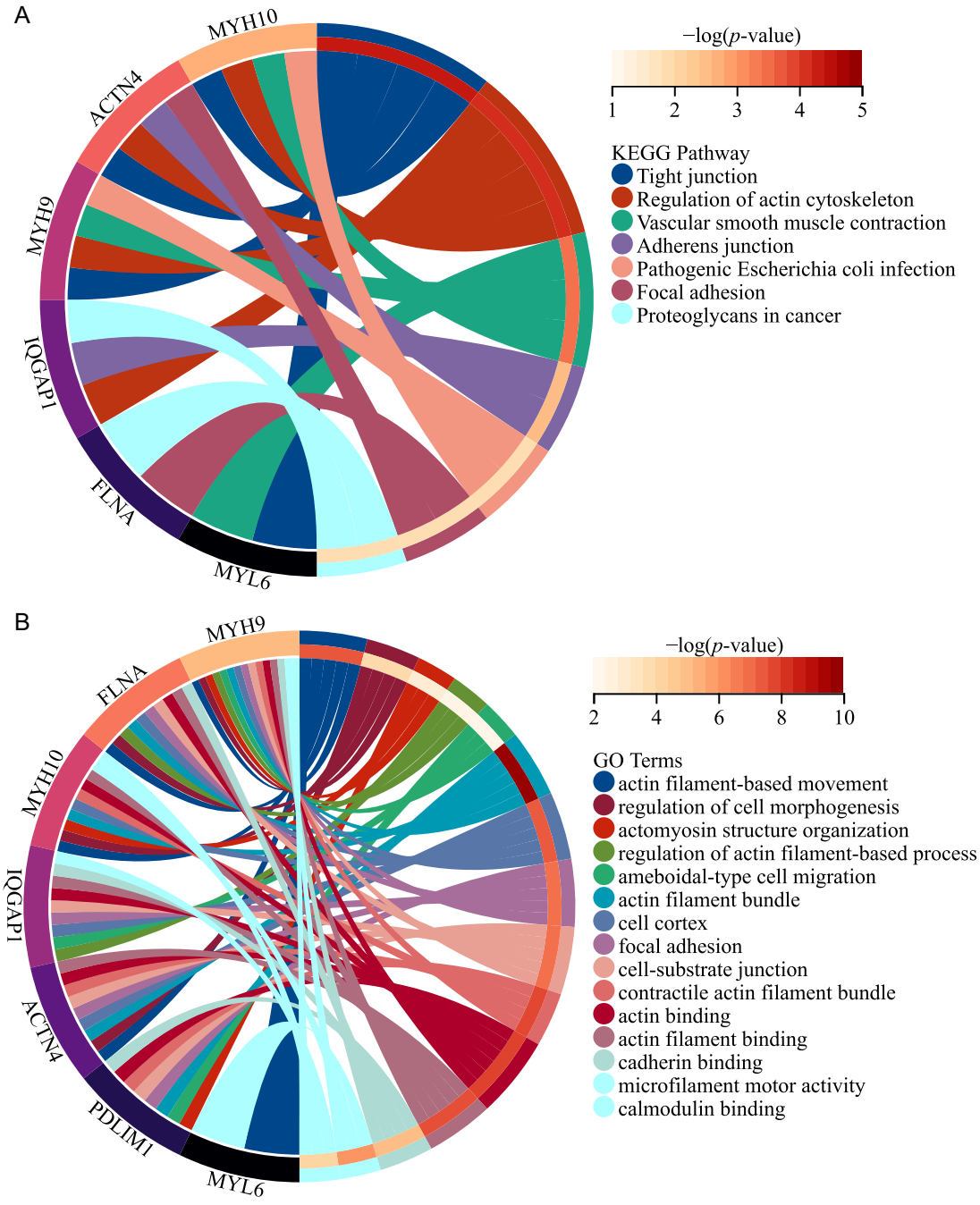

Fig. 3. Functional enrichment analysis. (A) KEGG pathway enrichment results highlighting significant pathways associated with DR-DEGs. (B) GO pathway analysis results showing the distribution of DR-DEGs in BP, CC, and MF.

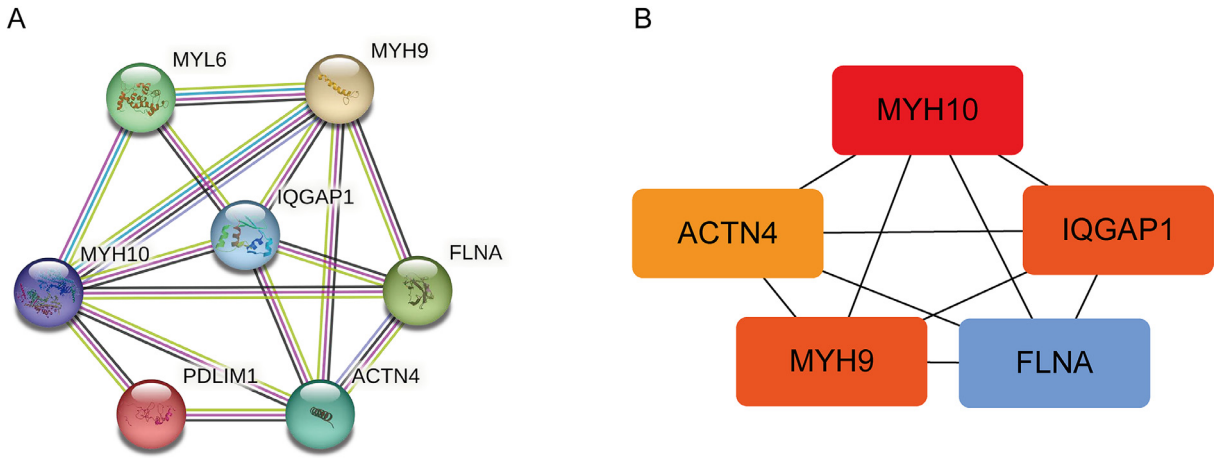

Fig. 4. Protein–protein interaction (PPI) network of DR-DEGs. (A) PPI network comprising 7 DR-DEGs illustrating their interactions. (B) Subnetwork highlighting the top five hub genes from the PPI network, determined using the maximum correlation criterion.

nodes were interrelated. Hub genes were identified using the cytoHubba plug-in. The top five hub genes were myosin heavy chain 10 (MYH10), alpha-actinin-4 (ACTN4), myosin heavy chain 9 (MYH9), filamin-A (FLNA) and Iq motif containing GTPase activating protein 1 (IQGAP1) (Fig. 4B).

3.4. Immune cell infiltration status between sepsis and control

The landscape of related immune cell infiltration and immune function was analyzed using the ssGSEA algorithm. Fig. 5A shows the expression status of 16 immune cells and 13 immune-related pathways across all patients. Fig. 5B shows the expression of 16 immune cells in the sepsis and control groups. Thirteen immune cells displayed significant differences in expression between the control and sepsis groups. The numbers of activated dendritic cells (aDCs), B cells, $CD8^+$ T cells, immature dendritic cells (iDCs), natural killer (NK) cells, plasmacytoid dendritic cells (pDCs), T helper cells, follicular helper T cells (Tfh), Th1 cells, Th2 cells, and tumor-infiltrating lymphocytes (TILs) were significantly lower in the sepsis group than in the control group. Conversely, the numbers of macrophages and regulatory T cells (Tregs) were significantly higher in the sepsis group. As shown in Fig. 5C, the levels of antigen-presenting cell (APC) co-stimulation, CC chemokine receptor (CCR), checkpoint markers, cytolytic activity, human leukocyte antigen (HLA), inflammation promotion, major histocompatibility complex (MHC) class I, T-cell co-inhibition, T-cell co-stimulation, and type II interferon (IFN) response were significantly lower in the sepsis group compared to the control group. The expression level of APC co-inhibition was significantly higher in the sepsis group. The correlation between immune cell infiltration (IMCs) and immune function (IMFs) is shown in Fig. 5D and E. A strong positive correlation was observed between TILs and Th1 cells (correlation coefficient = 0.8), while a strong negative correlation was seen between TILs and macrophages (correlation coefficient = −0.65). The positive correlation between parainflammation and type I IFN response was the strongest (correlation coefficient = 0.93), whereas the strongest negative correlation was observed between T-cell co-stimulation and APC co-inhibition (correlation coefficient = −0.23). Fig. 5F shows that five hub genes were significantly correlated with IMCs/IMFs. MYH10 was negatively correlated with IMCs/IMFs, while FLNA, ACTN4, MYH9, and IQGAP1 were positively correlated with immune components.

3.5. Risk model of the IHGs: establishment and validation

A predictive nomogram model for sepsis was constructed to estimate the diagnostic potential of IHGs (Fig. 6A). The AUC of the model used to depict the nomogram was 0.917 (Fig. 6B). The calibration curve used to verify the the nomogram's effectiveness revealed strong consistency between the actual and predicted probabilities (Fig. 6C). A high C-index value of 0.897 was achieved in interval validation (Fig. 6D). The calibration curve for the validation set is shown in Fig. 6E.

3.6. Related miRNA-IHGs regulatory network analysis

A miRNA regulatory network was constructed based on IHGs using the TargetScan database. The network consisted of 17 nodes (5 genes, 12 miRNAs) and 27 edges (Fig. 7). Within the network, both has-miR-1538 and has-miR-4745-3p were associated with ACTN4, MYH9, and MYH10. In addition, MYH9 was regulated by the majority of the miRNAs.

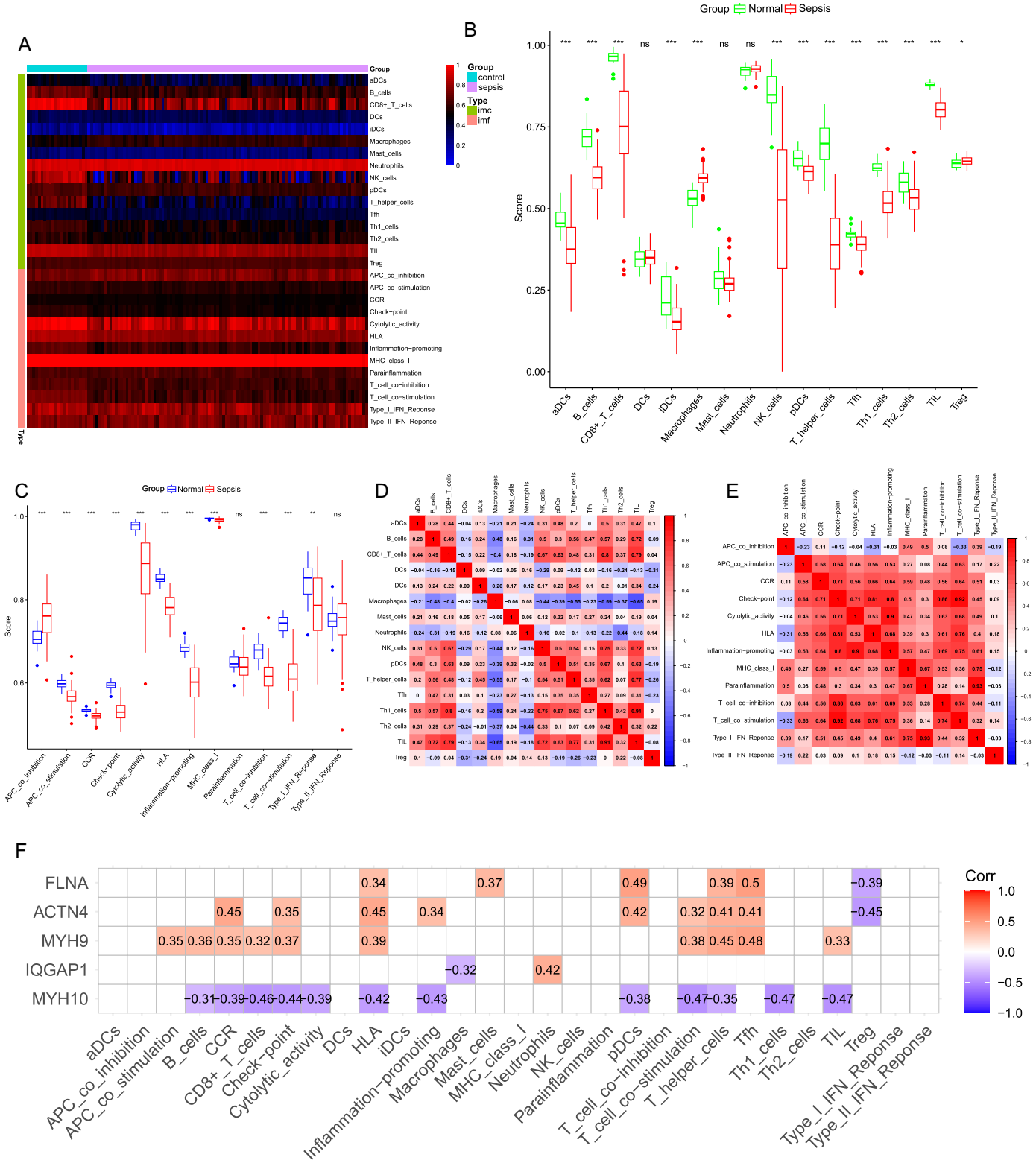

Fig. 5. Landscape of immune cell infiltration status between sepsis and control cohorts in the GSE95233 training set. (A) Heatmap showing the distribution of IMCs and IMFs across the samples. Blue areas represent the 22 control group samples, while purple areas represent the 102 sepsis group samples. Box plots showing differences in (B) immune cell infiltration and (C) immune function between sepsis and normal cohorts. Correlation matrix for (D) 16 immune cell subtypes and (E) 13 immune-related pathways. (F) Heatmap illustrating the correlation between immune-related hub genes and immune infiltration status. $^{*}p<0.05$, $^{**}p<0.01$, and $^{***}p<0.001$.

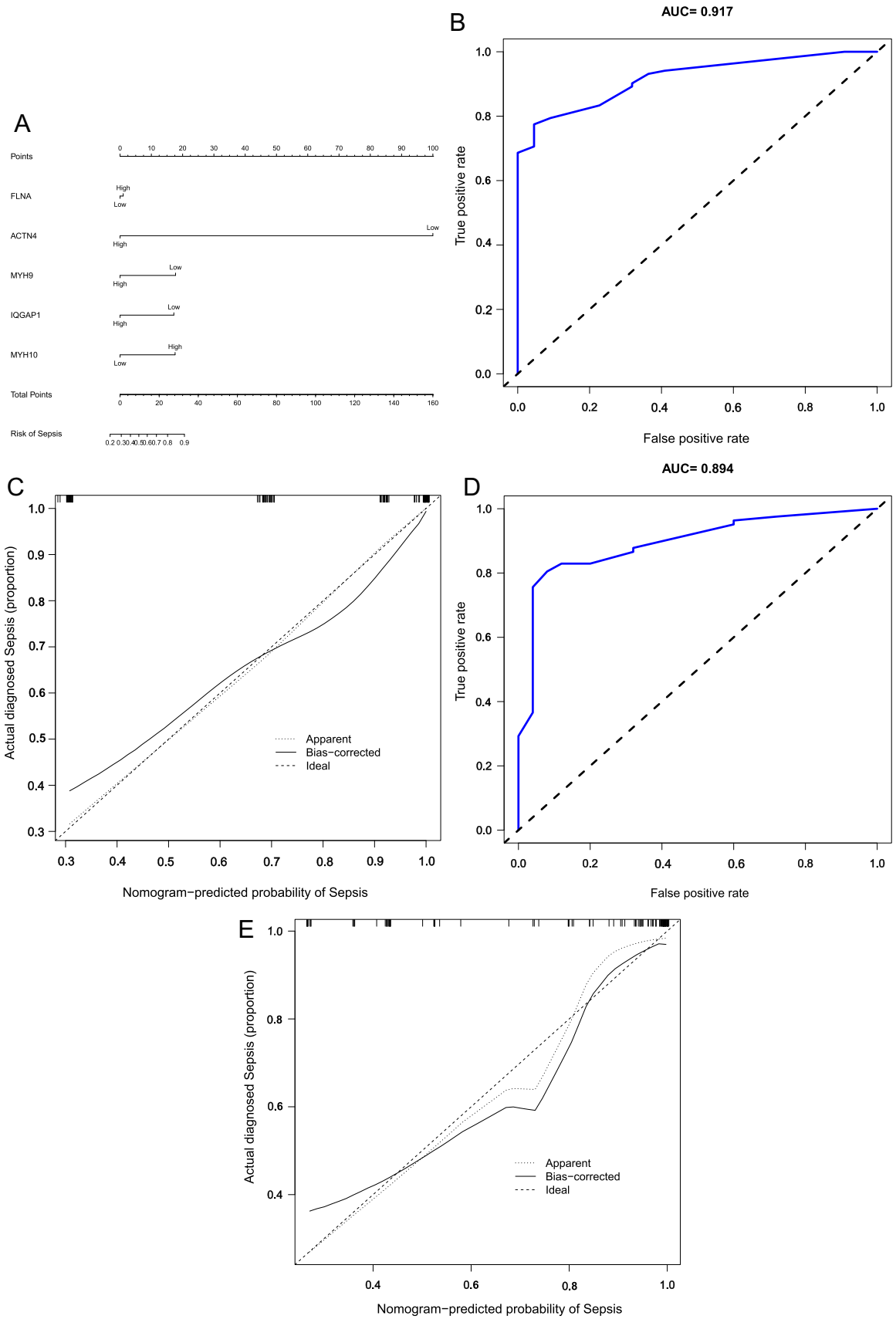

Fig. 6. Nomogram of immune-related hub genes and ROC curves and calibration curve of the nomogram for predicting the risk of sepsis. (A) Nomogram based on the expression levels of FLNA, ACTN4, MYH9, IQGAP1, and MYH10 for diagnosing sepsis. (B) ROC curve for the nomogram, illustrating its diagnostic accuracy. (C) Calibration curve for the nomogram, with the 45-degree dotted line indicating perfect prediction. (D) ROC curve for the validation cohort, confirming the nomogram's predictive ability. (E) Calibration curve for the validation cohort, demonstrating prediction reliability.

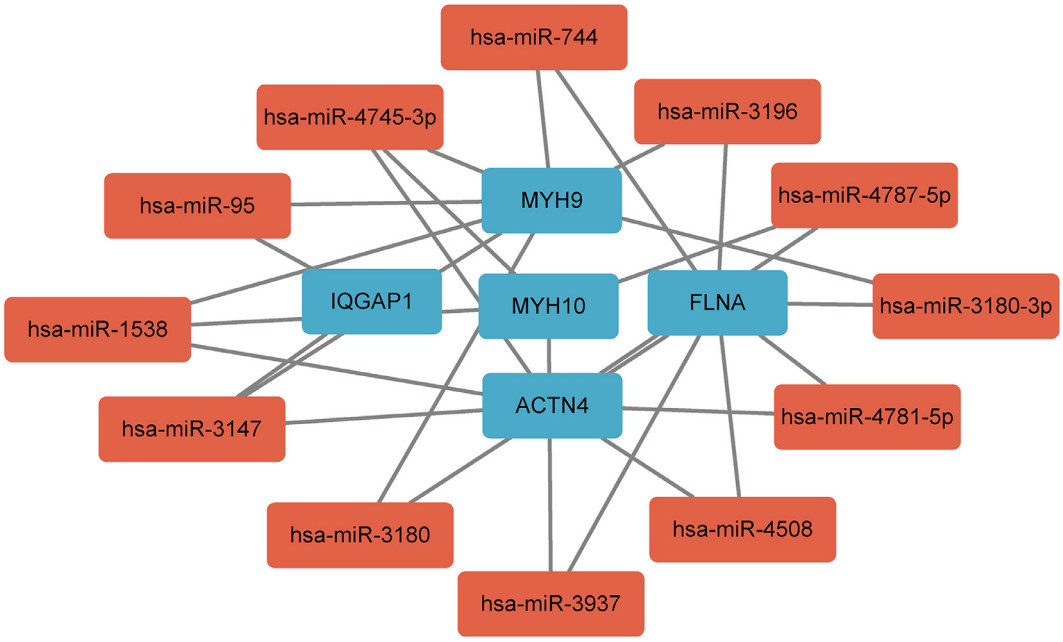

Fig. 7. Regulatory network of key miRNAs and target genes. The red rectangles represent miRNAs, and the blue circles represent target genes, highlighting the interaction between miRNAs and immune-related hub genes.

4. Discussion

Sepsis has high morbidity and mortality rates worldwide, especially in developing countries, accounting for an estimated 20% of all global deaths [13]. Sepsis can activate various forms of cell death [14], and increasing research is focused on understanding the types of cell death involved in sepsis. The pathology of disulfidptosis shares some characteristics with sepsis, such as alterations in actin dynamics. In this study, we analyzed the differences in disulfidptosis-related DEGs between sepsis patients and healthy controls. Seven DR-DEGs were identified, including two upregulated and five downregulated genes, followed by functional enrichment and pathway analyses. We then focused on immune cell infiltration status and found that cellular immunity and antigen presentation were primarily upregulated in the sepsis cohort. Through correlation analysis of IMCs, IMFs, and hub genes, we identified five IHGs and constructed a nomogram, ROC curve, calibration curve, and miRNA-IHGs regulatory network. The diagnostic value of these IHGs were also validated in a separate cohort.

In this study, we found that DEGs were mainly enriched in pathways associated with actin dynamics. Previous studies have shown that small GTPase family members, such as RhoA, regulate actin dynamics, and the actomyosin cytoskeleton is directly influenced by molecules like Rho kinases during sepsis [15]. Increased vascular permeability is a hallmark of sepsis [16], and dynamic alterations in actin fiber formation play an important role in hyperpermeability. Activated protein C, which induces dynamic rearrangement of the endothelial cell actin cytoskeleton, has been used to treat severe sepsis to protect the endothelial barrier [17]. In an adult rat model of severe sepsis, Rho-kinase signaling plays a role in the adhesive and mechanical mechanisms of septic lung injury [18]. The enhanced activity of the RhoA/ROCK pathway contributes to vasoconstriction by increasing responsiveness to angiotensin II in sepsis-surviving rats [19]. F-actin was also found useful for risk stratification in patients with symptoms of sepsis [20]. Disulfidptosis, a newly discovered form of programmed cell death described by Chen et al. relies on the susceptibility of the actin cytoskeleton to disulfide stress [4]. These studies collectively emphasize the importance of actin dynamics in sepsis, suggesting that the RhoA/ROCK pathway may play a crucial role in the pathophysiology of the condition.

The disruption of immune homeostasis is a crucial aspect of organ dysfunction in sepsis. Sepsis impacts the immune system by directly altering the lifespan, production, and function of effector cells responsible for maintaining homeostasis [21]. Maintaining immune balance is a potential research direction for developing clinical cure. Our study showed that Tregs and macrophages were highly expressed in the sepsis group. Tregs are major immunoregulatory cells derived from naïve T cells [22]. Numerous studies have demonstrated that forkhead box P3 (FOXP3) regulates Treg cell development, function, and homeostasis by activating or inhibiting its target genes [23,24]. Various factors can modulate Treg function by phosphorylating different sites of FOXP3 [25]. In addition, the resolution of inflammation in sepsis is controlled by multiple subsets of regulatory immune cells, including Tregs. A study by Shigeaki Inoue on a cecal slurry-induced septic mouse model showed that infiltrated Tregs can alleviate sepsis-associated encephalopa-

thy by reducing neuroinflammation [26]. Macrophages can be classified into two main phenotypes: inflammatory or classically activated (M1-like) macrophages, and healing or alternatively activated (M2-like) macrophages [27]. M1-like macrophages secrete large amounts of proinflammatory mediators, whereas M2-like macrophages secrete anti-inflammatory mediators [28]. Increasingly, studies focus on targeted drugs to regulate immune balance in sepsis treatment rather than relying solely on traditional antibiotics. Wang et al. demonstrated that silencing IncRNA-Cox2 modulated macrophage polarization by inhibiting the CREB-C/EBPβ pathway, thereby retaining sepsis progression [29]. Carestia et al. showed that platelets can promote macrophage polarization towards the M1 phenotype, improving sepsis outcomes [30]. Our analysis revealed that aDCs, B cells, $CD8^+$ T cells, iDCs, NK cells, pDCs, T helper cells, Tfh cells, Th1 cells, Th2 cells and TILs were downregulated in sepsis patients. Unlike macrophages, NK cells and DCs showed a decline in numbers and basic function early after infection [31,32], and lymphocytes, including B cells and $CD8^+$ T cells, was markedly reduced due to their susceptibility to apoptosis [33]. Yao et al. found that DCs exhibited low proliferative and self-renewal abilities compared to other immune cell types during sepsis [34].

We identified five DR-DEGs as immune-related hub genes: MYH10, FLNA, ACTN4, MYH9, and IQGAP1. MYH10 was negatively correlated with the differential IMCs and IMFs, whereas FLNA, ACTN4, MYH9, and IQGAP1 were mostly positively associated with immune components. These five genes were validated in both the training and validation sets. Few studies have explored the relationship between MYH10 and sepsis. In contrast to our findings, MYH9 and MYH10 have been shown to cooperate in chronic kidney disease and cancer [35,36]. As non-muscle myosin II complexes, MYH9 and MYH10 are key regulators of actin dynamics [37]. MYH9 regulates cell shape, while MYH10 regulates the activation state of microglia [38]. FLNA, a member of the filamin family, is a large dimeric actin-binding protein that stabilizes the actin fiber network [39]. Research has demonstrated that FLNA mutants can regulate actin dynamics via Rho GTPases, which control monocyte migration [40]. ACTN4 is a non-muscle alpha-actinin belonging to the actin-binding protein family [41]. Studies have shown that ACTN4 expression is associated with tumor growth and metastasis due to its role in the cytoskeleton [42,43]. IQGAP1, a scaffold protein interacting with cytoskeletal components and cell adhesion molecules, regulates actin and cell migration by modulating Rho GTPases, increasing cancer cells motility [44]. Collectively, these five hub genes are associated with actin dynamics, and most have been implicated in tumorigenesis. Based on the miRNA-IHGs regulatory network, MYH9 plays a crucial role in the early diagnosis of sepsis. MYH9, as a key factor in actin-based cell motility, is closely related to fibroblast-dominant pathology [45]. Studies have shown that MYH9 is a key regulator of tumor-like invasion and migration of fibroblast-like synoviocytes in patients with rheumatoid arthritis [46]. We propose that MYH9 may play a significant role in sepsis by influencing migration and invasion pathology.

The study has several limitations. The results require confirmation through clinical trials and experiments, as all data were derived from public databases. Future studies should involve more rigorous experimental designs to validate the function and therapeutic potential of DR-DEGs in sepsis.

5. Conclusion

In this study, we uncovered the relationship between disulfidptosis-related genes and immune infiltration status in sepsis. Based on the five selected hub genes, we validated their diagnostic value and constructed a regulatory network underlying sepsis. Further studies are necessary to explore the role of disulfidptosis in sepsis more comprehensively.

Funding

This study was supported by the Clinical Research Project of Shandong University, 2021 (2021SDUCRCC004).

CRediT authorship contribution statement

Wenlu Zou: acquisition of data, statistical analysis technical and interpretation of data, drafting of the manuscript, analysis and interpretation of data, critical revision of the manuscript for important intellectual content.

Lintao Sai, Sai Wen and Li Song: acquisition of data, material support, technical, and administrative.

Gang Wang: study concept and design, critical revision of the manuscript for important intellectual content, and administrative.

Acknowledgments

I would like to express my gratitude to Dr. Xu Nannan for her invaluable guidance and support throughout the writing of this paper.

Declaration of competing interest

The authors declare that they have no known competing financial interests or personal relationships that could have appeared to influence the work reported in this paper.

Data available statement

The microarray datasets during this study were downloaded from the NCBI Gene Expression Omnibus (https://www.ncbi.nlm.nih.gov/geo/query/acc.cgi?acc=GSE95233; https://www.ncbi.nlm.nih.gov/geo/query/acc.cgi?acc=GSE57065).

Ethics statement

Not applicable.

Informed consent

Not applicable.

References

[1] M. Huang, S. Cai, J. Su, The pathogenesis of sepsis and potential therapeutic targets, Int J Mol Sci 20 (21) (2019) 5376, doi:10.3390/ijms20215376.

[2] M. Cecconi, L. Evans, M. Levy, et al., Sepsis and septic shock, Lancet 392 (10141) (2018) 75–87, doi:10.1016/S0140-6736(18)30696-2.

[3] J.B. Belsky, E.P. Rivers, M.R. Filbin, et al., Thymosin beta 4 regulation of actin in sepsis, Expert Opin Biol Ther 18 (sup1) (2018) 193–197, doi:10.1080/14712598.2018.1448381.

[4] X. Liu, L. Nie, Y. Zhang, et al., Actin cytoskeleton vulnerability to disulfide stress mediates disulfidptosis, Nat Cell Biol 25 (2023) 404–414, doi:10.1038/s41556-023-01091-2.

[5] T. Wang, K. Guo, D. Zhang, et al., Disulfidptosis classification of hepatocellular carcinoma reveals correlation with clinical prognosis and immune profile, Int Immunopharmacol 120 (2023) 110368, doi:10.1016/j.intimp.2023.110368.

[6] P. Zheng, C. Zhou, Y. Ding, et al., Disulfidptosis: a new target for metabolic cancer therapy, J Exp Clin Cancer Res 42 (1) (2023) 103, doi:10.1186/s13046-023-02675-4.

[7] S. Zhao, L. Wang, W. Ding, et al., Crosstalk of disulfidptosis-related subtypes, establishment of a prognostic signature and immune infiltration characteristics in bladder cancer based on a machine learning survival framework, Front Endocrinol 14 (2023) 1180404, doi:10.3389/fendo.2023.1180404.

[8] D.A.C. Messerer, H. Schmidt, M. Frick, et al., Ion and water transport in neutrophil granulocytes and its impairment during sepsis, Int J Mol Sci 22 (4) (2021) 1699, doi:10.3390/ijms22041699.

[9] J.B. Belsky, M.R. Filbin, E.P. Rivers, et al., F-Actin is associated with a worsening qSOFA score and intensive care unit admission in emergency department patients at risk for sepsis, Biomarkers 25 (5) (2020) 391–396, doi:10.1080/1354750X.2020.1771419.

[10] Z. Ding, F. Du, C.F. Rönnow, et al., Actin-related protein 2/3 complex regulates neutrophil extracellular trap expulsion and lung damage in abdominal sepsis, Am J Physiol Lung Cell Mol Physiol 322 (5) (2022) L662–L672, doi:10.1152/ajplung.00318.2021.

[11] E. Clough, T. Barrett, The gene expression omnibus database, Methods Mol Biol 1418 (2016) 93–110, doi:10.1007/978-1-4939-3578-9_5.

[12] M.E. Ritchie, B. Phipson, D. Wu, et al., Limma powers differential expression analyses for RNA-sequencing and microarray studies, Nucleic Acids Res 43 (7) (2015) e47, doi:10.1093/nar/gkv007.

[13] K.E. Rudd, S.C. Johnson, K.M. Agesa, et al., Global, regional, and national sepsis incidence and mortality, 1990-2017: analysis for the Global Burden of Disease Study, Lancet 395 (10219) (2020) 200–211, doi:10.1016/S0140-6736(19)32989-7.

[14] C. Lelubre, J.L. Vincent, Mechanisms and treatment of organ failure in sepsis, Nat Rev Nephrol 14 (2018) 417–427, doi:10.1038/s41581-018-0005-7.

[15] M. Schnoor, A. García Ponce, E. Vadillo, et al., Actin dynamics in the regulation of endothelial barrier functions and neutrophil recruitment during endotoxemia and sepsis, Cell Mol Life Sci 74 (11) (2017) 1985–1997, doi:10.1007/s00018-016-2449-x.

[16] W.L. Lee, A.S. Slutsky, Sepsis and endothelial permeability, N Engl J Med 363 (7) (2010) 689–691, doi:10.1056/NEJMcibr1007320.

[17] J.R. Jacobson, J.G.N. Garcia, Novel therapies for microvascular permeability in sepsis, Curr Drug Targets 8 (4) (2007) 509–514, doi:10.2174/138945007780362719.

[18] K. Palani, M. Rahman, Z. Hasan, et al., Rho-kinase regulates adhesive and mechanical mechanisms of pulmonary recruitment of neutrophils in abdominal sepsis, Eur J Pharmacol 682 (1–3) (2012) 181–187, doi:10.1016/j.ejphar.2012.02.022.

[19] P. de Souza, K.L. Guarido, K. Scheschowitsch, et al., Impaired vascular function in sepsis-surviving rats mediated by oxidative stress and Rho-Kinase pathway, Redox Biol 10 (2016) 140–147, doi:10.1016/j.redox.2016.09.016.

[20] J.E. Gotts, M.A. Matthay, Sepsis: pathophysiology and clinical management, BMJ 353 (2016) i1585, doi:10.1136/bmj.i1585.

[21] M. Bosmann, P.A. Ward, The inflammatory response in sepsis, Trends Immunol 34 (3) (2013) 129–136, doi:10.1016/j.it.2012.09.004.

[22] Q.P. Nguyen, T.Z. Deng, D.A. Witherden, et al., Origins of CD4$^+$ circulating and tissue-resident memory T-cells, Immunology 157 (1) (2019) 3–12, doi:10.1111/imm.13059.

[23] Y. Zheng, S.Z. Josefowicz, A. Kas, et al., Genome-wide analysis of Foxp3 target genes in developing and mature regulatory T cells, Nature 445 (7130) (2007) 936–940, doi:10.1038/nature05563.

[24] N. Ohkura, S. Sakaguchi, Transcriptional and epigenetic basis of Treg cell development and function: its genetic anomalies or variations in autoimmune diseases, Cell Res 30 (2020) 465–474, doi:10.1038/s41422-020-0324-7.

[25] G. Deng, X. Song, S. Fujimoto, et al., Foxp3 post-translational modifications and Treg suppressive activity, Front Immunol 10 (2019) 2486, doi:10.3389/fimmu.2019.02486.

[26] M. Saito, Y. Fujinami, Y. Ono, et al., Infiltrated regulatory T cells and Th2 cells in the brain contribute to attenuation of sepsis-associated encephalopathy and alleviation of mental impairments in mice with polymicrobial sepsis, Brain Behav Immun 92 (2021) 25–38, doi:10.1016/j.bbi.2020.11.010.

[27] U. Patel, S. Rajasingh, S. Samanta, et al., Macrophage polarization in response to epigenetic modifiers during infection and inflammation, Drug Discov Today 22 (1) (2017) 186–193, doi:10.1016/j.drudis.2016.08.006.

[28] X. Chen, Y. Liu, Y. Gao, et al., The roles of macrophage polarization in the host immune response to sepsis, Int Immunopharmacol 96 (2021) 107791, doi:10.1016/j.intimp.2021.107791.

[29] Q. Wang, Y. Xie, Q. He, et al., LncRNA-Cox2 regulates macrophage polarization and inflammatory response through the CREB-C/EBPβ signaling pathway in septic mice, Int Immunopharmacol 101 (2021) 108347, doi:10.1016/j.intimp.2021.108347.

[30] A. Carestia, H.A. Mena, C.M. Olexen, et al., Platelets promote macrophage polarization toward pro-inflammatory phenotype and increase survival of septic mice, Cell Rep 28 (4) (2019) 896–908.e5, doi:10.1016/j.celrep.2019.06.062.

[31] P. Hohlstein, H. Gussen, M. Bartneck, et al., Prognostic relevance of altered lymphocyte subpopulations in critical illness and sepsis, J Clin Med 8 (3) (2019) 353, doi:10.3390/jcm8030353.

[32] I.J. Jensen, C.S. Winborn, M.G. Fosdick, et al., Polymicrobial sepsis influences NK-cell-mediated immunity by diminishing NK-cell-intrinsic receptor-mediated effector responses to viral ligands or infections, PLoS Pathog 14 (10) (2018) e1007405, doi:10.1371/journal.ppat.1007405.

[33] M.D. Martin, V.P. Badovinac, T.S. Griffith, CD4 T cell responses and the sepsis-induced immunoparalysis state, Front Immunol 11 (2020) 1364, doi:10.3389/fimmu.2020.01364.

[34] R.Q. Yao, Z.X. Li, L.X. Wang, et al., Single-cell transcriptome profiling of the immune space-time landscape reveals dendritic cell regulatory program in polymicrobial sepsis, Theranostics 12 (10) (2022) 4606–4628, doi:10.7150/thno.72760.

[35] K.L. Otterpohl, B.W. Busselman, I. Ratnayake, et al., Conditional Myh9 and Myh10 inactivation in adult mouse renal epithelium results in progressive kidney disease, JCI Insight 5 (21) (2020) e138530, doi:10.1172/jci.insight.138530.

[36] L. Liu, C. Chen, P. Liu, et al., MYH10 combines with MYH9 to recruit USP45 by deubiquitinating snail and promotes serous ovarian cancer carcinogenesis, progression, and cisplatin resistance, Adv Sci 10 (14) (2023) e2203423, doi:10.1002/advs.202203423.

[37] A.M. Holtz, R. VanCoillie, E.A. Vansickle, et al., Heterozygous variants in MYH10 associated with neurodevelopmental disorders and congenital anomalies with evidence for primary cilia-dependent defects in Hedgehog signaling, Genet Med 24 (10) (2022) 2065–2078, doi:10.1016/j.gim.2022.07.005.

[38] P.N. Melo, M. Souza da Silveira, I. Mendes Pinto, et al., Morphofunctional programming of microglia requires distinct roles of type II myosins, Glia 69 (11) (2021) 2717–2738, doi:10.1002/glia.24067.

[39] J.P. Rosa, H. Raslova, M. Bryckaert, Filamin A: key actor in platelet biology, Blood 134 (16) (2019) 1279–1288, doi:10.1182/blood.2019000014.

[40] R. Leung, Y. Wang, K. Cuddy, et al., Filamin A regulates monocyte migration through Rho small GTPases during osteoclastogenesis, J Bone Miner Res 25 (5) (2010) 1077–1091, doi:10.1359/jbmr.091114.

[41] D. Tentler, E. Lomert, K. Novitskaya, et al., Role of ACTN4 in tumorigenesis, metastasis, and EMT, Cells 8 (11) (2019) 1427, doi:10.3390/cells8111427.

[42] Y.Y. Zhang, H. Tabataba, X.Y. Liu, et al., ACTN4 regulates the stability of RIPK1 in melanoma, Oncogene 37 (29) (2018) 4033–4045, doi:10.1038/s41388-018-0260-x.

[43] Q. Chen, H. Wang, Z. Li, et al., Circular RNA ACTN4 promotes intrahepatic cholangiocarcinoma progression by recruiting YBX1 to initiate FZD7 transcription, J Hepatol 76 (1) (2022) 135–147, doi:10.1016/j.jhep.2021.08.027.

[44] X. Peng, T. Wang, H. Gao, et al., The interplay between IQGAP1 and small GTPases in cancer metastasis, Biomed Pharmacother 135 (2021) 111243, doi:10.1016/j.biopha.2021.111243.

[45] M. Vicente-Manzanares, X. Ma, R.S. Adelstein, et al., Non-muscle myosin II takes centre stage in cell adhesion and migration, Nat Rev Mol Cell Biol 10 (11) (2009) 778–790, doi:10.1038/nrm2786.

[46] S. Lee, E. Choi, S. Chae, et al., Identification of MYH9 as a key regulator for synoviocyte migration and invasion through secretome profiling, Ann Rheum Dis 82 (8) (2023) 1035–1048, doi:10.1136/ard-2022-223625.